Clinical Neurophysiology 127 (2016) 1088–1098

Contents lists available at ScienceDirect

Clinical Neurophysiology

journal homepage: www.elsevier.com/locate/clinph

# Single Pulse Electrical Stimulation to identify epileptogenic cortex: Clinical information obtained from early evoked responses

B.E. Mouthaan [a,b,1], M.A. van 't Klooster [a,*,1], D. Keizer [a,b], G.J. Hebbink [a,b], F.S.S. Leijten [a], C.H. Ferrier [a], M.J.A.M. van Putten [b], M. Zijlmans [a,c], G.J.M. Huiskamp [a]

[a] Brain Center Rudolf Magnus, Department of Neurology and Neurosurgery, University Medical Center Utrecht, Utrecht, The Netherlands
[b] MIRA, Institute for Biomedical Technology and Technical Medicine, University of Twente, Enschede, The Netherlands
[c] SEIN – Stichting Epilepsie Instellingen Nederland, Heemstede, The Netherlands

ARTICLE INFO

*Article history:*
Accepted 27 July 2015
Available online 20 August 2015

*Keywords:*
Epilepsy surgery
Electrical stimulation
Evoked potentials
Intracranial electrodes
High frequency oscillations

HIGHLIGHTS

- Electrodes with ERs are stronger associated with SOZ than with non-SOZ electrodes.
- Stimulating the SOZ evokes ERs that are associated with the seizure propagation area.
- ERs evoked by SPES can add information for identification of epileptic cortex.

ABSTRACT

*Objective:* Single Pulse Electrical Stimulation (SPES) probes epileptogenic cortex during electrocorticography. Two SPES responses are described: pathological delayed responses (DR, >100 ms) associated with the seizure onset zone (SOZ) and physiological early responses (ER, <100 ms) that map cortical connectivity. We analyzed properties of ERs, including frequencies >80 Hz, in the SOZ and seizure propagation areas.
*Methods:* We used data from 12 refractory epilepsy patients. SPES consisted of 10 pulses of 1 ms, 4–8 mA and 5 s interval on adjacent electrodes pairs. Data were available at 2048 samples/s for six and 512 samples/s (22 bits) for eight patients and analyzed in the time–frequency (TF) and time-domain (TD).
*Results:* Electrodes with ERs were stronger associated with SOZ than non-SOZ electrodes. ERs with frequency content >80 Hz exist and are specific for SOZ channels. ERs evoked by stimulation of seizure onset electrodes were associated with electrodes involved in seizure propagation.
*Conclusion:* Analysis of ERs can reveal aspects of pathology, manifested by association with seizure propagation and areas with high ER numbers that coincide with the SOZ.
*Significance:* Not only DRs, but also ERs could have clinical value for mapping epileptogenic cortex and help to unravel aspects of the epileptic network.


## 1. Introduction

Cortical Single Pulse Electrical Stimulation (SPES) and its responses yield information about the epileptic tissue in the brain. SPES was first described by Valentín et al. (2002) in focal refractory epilepsy patients who underwent chronic electrocorticography (ECoG) preceding surgery. The stimulation protocol consists of ten brief pulses of 1 ms and 4–8 mA amplitude with a 5 s interval given over two neighboring electrodes (Valentín et al., 2002). SPES evokes two types of responses: early responses (ERs) within 100 ms after stimulation and delayed responses (DRs) after 100 ms up to 1 s after stimulation (Valentín et al., 2002; Valentín et al., 2005a,b). SPES research has mainly focused on DRs. DRs are associated with the seizure onset zone (SOZ) and contain pathological high frequency (80–500 Hz) information. These high frequency DRs are more specific for the seizure onset zone compared to DRs in the low frequency band (<80 Hz) (van 't Klooster et al., 2011). ERs are assumed to be a physiological phenomenon originating from stimulation of cortico-cortical association fibers

* Corresponding author at: Brain Center Rudolf Magnus, Department of Neurology and Neurosurgery, University Medical Center Utrecht, PO Box 85500, 3584 CX Utrecht, The Netherlands. Tel.: +31 88 755 87959.
*E-mail address:* m.a.vanhetklooster-2@umcutrecht.nl (M.A. van 't Klooster).
[1] These authors contributed equally.

http://dx.doi.org/10.1016/j.clinph.2015.07.031
1388-2457/

(u-fibers). ERs resemble the N1 potential in cortico-cortical evoked potentials (CCEP; general settings 0.3 ms pulses, 1 Hz, 1–15 mA, 20–70 stimuli averaged). The N1 potential provides information regarding cerebral functional connectivity (Matsumoto et al., 2005, 2007, 2012a,b; Lacruz et al., 2007; Iwasaki et al., 2010; Enatsu et al., 2012a,b). It has been suggested as a method for the identification of functional areas during surgery (Saito et al., 2014). As such, CCEPs, and ERs, may reveal regions of rich network connectivity. On the other hand, it has been shown that seizure propagation proceeds locally through neocortical cells as well as over longer distances through the deeper lying u-fibers that are stimulated by CCEP (Spencer, 1988; Alarcon et al., 1994). ERs might mirror these seizure propagation pathways, thus revealing an important aspect of the pathology of epilepsy.

We investigated ERs, including higher frequency responses above 80 Hz, evoked by stimulation out- and inside the seizure onset zone (SOZ) and analyzed their properties in the SOZ and in areas of seizure propagation, respectively. We used two approaches; analysis in the time–frequency (TF) domain of high temporal resolution data and analysis in the time-domain (TD) of high dynamic range data.

## 2. Methods

### 2.1. Patients

Data from 12 patients (5 males, mean age 19.7 years, range 8–42 years) with refractory epilepsy who underwent chronic ECoG preceding epilepsy surgery were used. All patients were admitted to the intensive epilepsy monitoring unit of the UMC Utrecht in the Netherlands in the period 2008–2012. SPES was routinely performed as a clinical protocol. SPES results were included in the medical decision making after visual inspection in line with recommendations of Valentín et al. (2002).

Monitoring time ranged from 3 to 8 days. All 12 patients underwent resective surgery of a presumed epileptic focus. Five patients had temporal, three had frontal, two had frontocentral, and two had parietal lobe epilepsy. Most patients were on multiple anti-epileptic drugs that were tapered during the registration. Patient information is summarized in Table 1.

The institutional ethical committee indicated that no explicit approval was necessary because of the retrospective character of this study, provided that data were coded and handled anonymously.

### 2.2. Electrocorticography data

Subdural grids and strips (Ad-Tech, Racine, Wisconsin, USA) were placed under general anesthesia, after craniotomy. The circular platinum electrodes, imbedded in silicon, had a contact surface of 4.2 $mm^2$ and an inter-electrode spacing of 1 cm. In two patients, additional depth electrodes were implanted with eight cylindrical contacts with 7.9 $mm^2$ contact surface and 5 mm inter-electrode distance. Electrode placement was based on clinical pre-operative diagnostics, covering both the suspected epileptogenic region(s) and eloquent areas. Electrode positions on the cortex were obtained by co-registration of post-implantation CT with preoperative 3D MRI images (Noordmans et al., 2002). The median number of implanted electrodes was 96 (range 88–120) per patient (Table 1).

### 2.3. Clinical information

Per patient a recording of a typical spontaneous clinical seizure was analyzed retrospectively by two neurologists (chosen from CF/FL/MZ). They were asked to mark independently; (1) the one electrode with the first ictal activity as the seizure onset electrode (SO-electrode), (2) all electrodes on which seizure propagation was found (SP-electrodes) within the first 30 s after initial onset. Ictal activity was defined as the first ECoG pattern consisting of rhythmic spikes, rhythmic sharp waves, recruiting gamma activity, regular or low-amplitude activity in the beta range prior to or coinciding with the clinical manifestation of the seizure (Alarcon, 1996). In case of a generalizing seizure, observers marked all electrodes showing ictal activity up to the point of generalization. Disagreement in the marked onset or propagation between two observers was solved in a consensus meeting. Additionally, a clinical SOZ area was defined, based on all recorded seizures from the total monitoring period (by FL/CF). This SOZ typically contained multiple electrodes.

### 2.4. Single pulse data acquisition

Single Pulse Electrical Stimulation (SPES) was performed using a manually controlled cortical stimulator (IRES 600 surgical, Micromed, Treviso, Italy). Monophasic SPES stimuli were given, ten pulses with a duration of 1 ms, separated by 5 s intervals, on pairs of adjacent electrodes. Stimulation was performed at an intensity of 8 mA and only in stimulation pairs where twitches or pain occurred the intensity was gradually reduced to as low as 4 mA. In six patients SPES was available at a high sampling rate of 2048 Hz and a hardware anti-aliasing filter of 538 Hz in a subset of 64 electrodes simultaneously (SD128, Micromed, Treviso, Italy). Subset selection was based on the monitoring result of previous days, and included the clinical SOZ. In eight patients SPES was sampled at 512 Hz (anti-aliasing filter 134 Hz) with a high dynamic range at 22 bits resolution, simultaneously in all implanted electrodes. In two patients both types of recordings were available. Data were recorded with respect to an extra-cranial reference. All recordings showed stimulus artifacts in most electrodes that needed to be dealt with. Electrodes with other artifacts were excluded from analysis.

### 2.5. Time–frequency processing of SPES

We used the same SPES datasets and a similar analytical approach as in our previous study on time–frequency analysis of evoked DRs (van 't Klooster et al., 2011). The aim of the current study is time–frequency analysis of evoked ERs instead of evoked DRs. To enable analysis of ERs we made the following methodological changes: (1) the time-interval of interest was changed to <100 ms, (2) time–frequency decomposition was based on Hilbert-Huang Transformation instead of Wavelet transform in order to create a higher time resolution, and (3) additional processing was required in order to obtain images similar to the Event Related Spectral Pertubation images (ERSPs) in the previous study (van 't Klooster et al., 2011). Further details are provided in the following sections.

#### 2.5.1. Preprocessing

Time frequency (TF) analysis was done only on data sampled at 2048 Hz. Preprocessing of the data files was performed in Matlab® (The MathWorks, Natick, MA) as described in our previous study (van 't Klooster et al., 2011). Preprocessing steps included: stimulus detection, epoching of the data and re-referencing to average reference. Re-referencing was performed in order to exclude contamination of the data by frequencies above 70 Hz, mostly muscle artifacts, which could be present in the extra-cranial common reference. Epochs with interval of [−1 s:1 s] covering pre-stimulus baseline were selected. This resulted into ten epochs for each stimulated electrode pair and all recorded response electrodes.

**Table 1**
Patient characteristics.

| Pt | TD/TF | M/F | Age (y) | Region | Side | Pathology | Total # electrodes | Monitoring period (days) | # Seizures (onset activity, types) | SOZ resected? | Outcome (1y) Engel class |
|---|---|---|---|---|---|---|---|---|---|---|---|
| 1 | TD + TF | M | 42 | T | L | MTS | 96 | 7 | 2 (focal gamma onset, 1 type) | Complete | I |
| 2* | TD + TF | F | 23 | T | L | Glioneural heterotopia | 96 | 6 | 6 (gamma burst onset, 1type) | Complete | I |
| 3 | TF | M | 9 | Fr | L | FCD | 96 (16 depth) | 5 | 12 (focal beta-gamma onset, 1 type) | Incomplete | IV |
| 4 | TF | F | 31 | T | R | MCD | 88 | 8 | 1 (gamma onset) | Complete | I |
| 5 | TF | F | 13 | FrC | L&R | TS | 96 | 8 | 6 (gamma burst onset, 1 type) | Incomplete (multiple tubers bilateral) | IV |
| 6 | TF | M | 8 | FrC | L | Tumor | 96 | 5 | >100 (gamma onset, 1 type) | Complete | I |
| 7 | TD | F | 17 | Fr | R | FCD | 120 | 3 | 6 (gamma onset, 1 type) | Complete | I |
| 8 | TD | M | 8 | P | R | FCD | 94 (6 depth) | 5 | 1 (gamma onset, 1 type) | Incomplete (eloquent regions) | I |
| 9 | TD | F | 18 | Fr | L | Reactive changes | 112 | 7 | 19 (gamma onset, 1 type) | Complete | I |
| 10 | TD | F | 15 | P | L | FCD | 96 | 5 | 3 (gamma onset, 1 type) | Incomplete | IV |
| 11 | TD | M | 26 | T | L | MTS | 120 | 6 | 6 (gamma onset, 1 type) | Complete | I |
| 12** | TD | F | 27 | T | L | MCD | 96 | 6 | 4 (gamma onset, 2 types) | Incomplete | IV |

TD/TF = analysis performed; TD = time domain analysis, TF = time–frequency analysis, F = female, M = male, Fr = frontal, T = temporal, C = central, FrC = fronto-central, P = parietal, L = left, R = right, TS = tuberous sclerosis, MCD = malformation of cortical development, FCD = focal cortical dysplasia, MTS = mesial temporal sclerosis. # Seizures = number of spontaneous clinical seizures, outcome (1y) = post-operative outcome after 1 year using the Engel classification. *Patient 2 had a number of different electrodes on a single strip from which the clinically identical seizures originated. We choose one of these electrodes as SO-electrode, this could explain the poorer results in this patient compared the other patients. **In patient 12 two separate onset zones were found. Only one seizure onset zone could be resected, therefore we selected a seizure of that type.

An additional steep low-pass finite impulse response filter with a cut-off frequency of 500 Hz ($f_{stop}$ = 520 Hz, $f_{pass}$ = 500 Hz, attenuation >60 dB/octave) was applied to limit any interference of higher frequencies.

### 2.5.2. Time–frequency decomposition

The Hilbert-Huang transform (HHT) was used to detect ERs in the proximity of the stimulus artifact. HHT allows time–frequency analysis with a high time resolution that prevents overlap of the artifact with the ER time-window <100 ms we are interested in (Huang and Wu, 2008). The Hilbert-Huang transform provides a decomposition of the signal into a finite number of components. These so-called "modes" are not directly related to a specific frequency band, but when combined they result in a coverage, albeit incomplete, of the time–frequency matrix. Frequencies not present in the modes are absent in this matrix and their power is automatically set to zero.

HHT was implemented in Matlab® (The MathWorks, Natick, MA) using a customized script that is freely available online (http://perso.ens-lyon.fr/patrick.flandrin/emd.html) (Rilling et al., 2003). Default values for stop criteria and number of iterations were used as described there. HHT time–frequency analysis (range 5–500 Hz) was performed for each epoch of each stimulus pair. The frequency and time resolution were set at 1 Hz and 0.488 ms. Each analysis resulted in a time–frequency matrix of 496 rows by 4096 columns.

### 2.5.3. Construction of time–frequency images

Color coded ERSP images were constructed from the time–frequency matrix (Delorme and Makeig, 2004). First, the data were smoothed using a 15 × 15 weighted Gaussian filter. ERSP images were then calculated by averaging each set of ten stimulus epochs, generating one ERSP image for each stimulus pair for each set of response electrodes (total # ERSP images = # pairs of stimulated electrodes × 64 recorded electrodes). Significance ($p < 0.05$) of spectral perturbations was determined by bootstrapping based on a pre-stimulus baseline interval [−1 s:−0.2 s]. Intensity values were expressed in power on a logarithmic power scale [−20 dB:20 dB]. Additional stimulus masking was performed, by constructing a template based on the symmetry of the HHT of the stimulus artifact. The template was subtracted in each image to mask the artifact and enable better visualization of ERs. A schematic overview of the TF analysis can be found in Fig. 1A.

### 2.5.4. Visual analysis of ERSP images

ERSP images were visually classified for events in three frequency bands, spike (S)<80 Hz, ripple (R) 80–250 Hz and fast ripple (FR) band (250–500 Hz) (van 't Klooster et al., 2011). The time interval of interest for ERs was defined as [0 s:0.1 s] after stimulation, based on the latency definitions by Valentín et al. (2002). To avoid bias in interpretation, the DR interval [0.15–1 s] was removed from the final image. ERs were defined as clusters of increased power (coded orange-red) that stand out from the baseline for the same frequency band. Classification of the ER responses in all ERSP images for all stimulus electrode pairs was performed independently by two observers (chosen from CF/JH/GH/BM) for each patient. Inter-observer agreement was calculated by Cohen's kappa (κ) using SPSS 21 software (IBM SPSS Statistics, Rel. 21.0 2012, Chicago; SPSS Inc.). The κ-scores were calculated separately for the S, R and FR events. A $\kappa > 0.4$ was considered as reasonable agreement (Zijlmans et al., 2002; van 't Klooster et al., 2011). Final counts of ERs in the spike, ripple and fast ripple band were based on consensus events of two observers. Datasets with $\kappa < 0.4$ for all frequency bands were excluded from analysis.

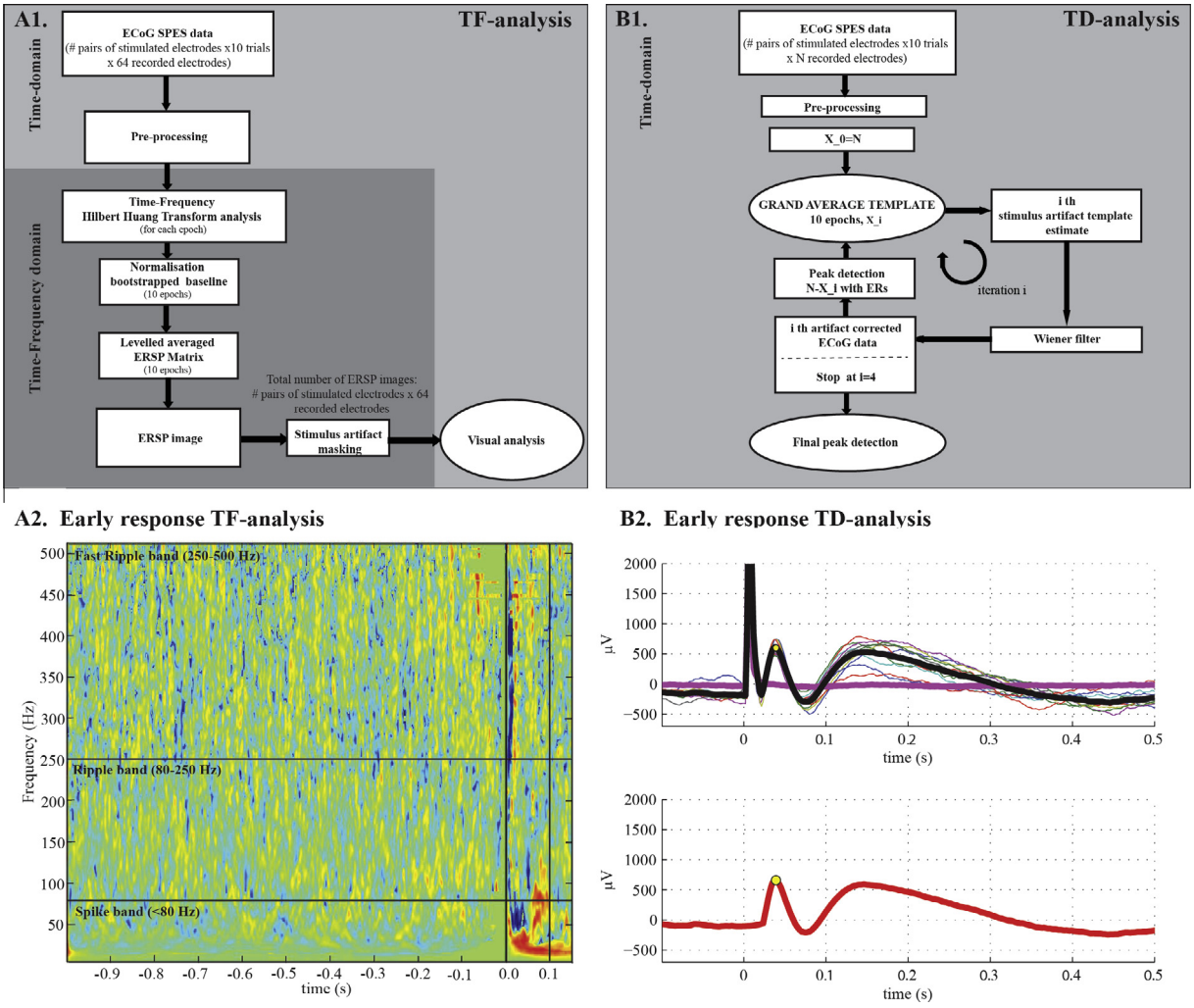


**Fig. 1.** Schematic representation of two analyses performed. (A1) TF analysis based on HHT constructed ERSP images. (A2) Resulting HHT based ERSP image of TF analysis, as presented to the observers. Red colors indicate enhanced power compared to the pre-stimulus baseline on a power scale of [−20:20] dB. Intense red (significantly increased power) = 20 dB, green (not significant) = 0 dB, and intense blue (significantly decreased power) = −20 dB. The vertical axis represents frequency, with the horizontal lines separating the S, R and FR frequency band. The horizontal axis is time, with the stimulus at $t = 0$. A pronounced spike and ripple event is shown around 50 ms after stimulation. (B1) TD analysis based on iterative Wiener filtering and peak detection of ER responses. (B2) TD analysis, thin lines are raw data for one electrode of responses evoked by 10 consecutive stimuli. The average is shown in black, the purple line shows the optimal Wiener filter estimate of the stimulus artifact. In the lower panel the artifact corrected average response (red) with the ER detected by the peak detection (yellow dot). (For interpretation of the references to color in this figure legend, the reader is referred to the web version of this article.)

### 2.6. Time-domain processing of SPES

#### 2.6.1. Preprocessing

Time domain (TD) analysis was done only for data recorded with high dynamic range (22 bits). These recordings contain all implanted electrodes, and include both the SOZ and the seizure propagation area. Preprocessing consisted of stimulus detection and epoching as described above, but no re-referencing was performed. For TD analysis, as opposed to TF analysis, contamination of frequencies above 70 Hz present in the extra-cranial common reference does not pose a problem.

#### 2.6.2. Artifact correction and event detection

An algorithm was developed to detect ERs in the time-domain consisting of two steps (Matlab®, The MathWorks, Natick, MA). Step 1 is removal of the stimulus artifact. This was based on Wiener filtering, assuming that the shape of the artifact is the same in all response electrodes for a given stimulus pair. A major determinant of the shape of the stimulus artifact in our data is cross-talk of the leads carrying the stimulus current to leads of recording channels in the same connecting cable. Therefore the stimulus artifact has generally the same shape, however, the amplitude may differ per electrode. First, a grand average over 10 pulses and over each response electrode was taken. Note that the large number of electrodes ($X_0 = N$, which ranges 80–120 electrodes) provides that the number of electrodes without ERs exceeds the number of electrodes with ERs, implying that this average is dominated by artifact data. Therefore it was used as the first template to construct a Wiener filter, which, when applied, removed the main part of the stimulation artifact. Next, ER responses were detected automatically in the filtered data by a quick peak detection algorithm (PeakFinder, N. Yoder, Matlab file-central). A more accurate template artifact was then constructed by excluding electrodes with ERs ($N$–$X_i$) from a new grand average over the original data. The new template was then again used for Wiener filtering. This process is repeated four times (iteration $i = 1{:}4$) to further refine the template artifact. Step 2 of the algorithm is the final ER peak detection in the interval 0.02–0.1 s after stimulation. This interval was chosen to avoid potential bias for incomplete artifact correction that interferes with the onset of the ER. For final peak detection the same algorithm as mentioned above was used, but now with an adaptive amplitude threshold determined by visual

inspection. The choice of amplitude threshold was made by favoring over-detection over under-detection; when visually clear responses were not adequately detected due to an inadequate threshold setting this was lowered by 10 μV steps. A schematic overview of the TD analysis can be found in Fig. 1B. ER response electrodes were those that exceeded the threshold for a particular stimulus electrode pair. For the TD analysis of ERs and seizure propagation, stimulation of a single electrode pair was considered: one electrode was the electrode marked as SO-electrode (see Section 2.3) and the other a neighboring electrode that was located on the same gyrus. In cases of ambiguity, the stimulation pair that showed the largest total number of responses was chosen.

### 2.7. Statistical analysis

Statistical analysis was performed in IBM SPSS Statistics 21 (IBM Corp., Armonk, NY, USA). For all tests we considered $p$-values <0.05 significant. TF analyses were done for the spike, ripple and fast ripple band separately. The following analyses were done for TF and TD, when appropriate.

#### 2.7.1. Early response counts

For the TF analysis we counted the number of ERs per electrode ($ER_{count}$) for the total of all stimulus pairs. We normalized the number of ERs in each response electrode with respect to the maximal count ($ER_{max}$) found, expressed as percentage:

$$ER_{norm} = (ER_{count}/ER_{max}) \times 100\% \quad (1)$$

We then defined electrodes with a high occurrence of ERs, $ER_{norm} > 50\%$, as $ER_{50}$ electrodes.

So while the detection of a single ER in a particular band reflects the excitability of the underlying tissue with respect to the stimulus, high values of $ER_{norm}$ will reflect the richness of connections to that electrode.

#### 2.7.2. Association of ER counts with SOZ and ERs with propagation

We tested for differences in the value of $ER_{norm}$ between SOZ and non-SOZ channels using a non-parametric Mann–Whitney $U$ test (two-tailed). Differences between association of $ER_{50}$ electrodes with SOZ and with non-SOZ channels was assessed using Fisher's exact test (two-tailed) (TF analysis). We tested for differences in association between ERs, following stimulation of SO-electrode, in SP-electrodes and non-SP-electrodes using Fisher's exact test (two-tailed) (TD analysis).

#### 2.7.3. Sensitivity and specificity of ERs

To further quantify results, sensitivity, specificity, positive and negative predictive value (PPV and NPV) of $ER_{50}$ for the clinical SOZ (TF analysis) and ER for seizure propagation (TD analysis) was determined. Sensitivity was calculated as tp/(tp + fn), specificity as tn/(tn + fp), PPV as (tp/tp + fp) and NPV as (tn/tn + fn).

For TF analysis an electrode was considered as:

- a true positive electrode (tp) if involved in the SOZ and classified as $ER_{50}$ electrode,
- a false positive electrode (fp) if NOT involved in the SOZ but classified as $ER_{50}$ electrode,
- a true negative electrode (tn) if NOT involved in the SOZ and NOT classified as $ER_{50}$ electrode, and
- a false negative electrode (fn) if involved in the SOZ but NOT classified as $ER_{50}$ electrode.

For TD analysis an electrode was considered as:

- a true positive electrode (tp) if marked as SP-electrode and showing ERs,
- a false positive electrode (fp) if NOT marked as SP-electrode but showing ERs,
- a true negative electrode (tn) if NOT marked as SP-electrode and NOT showing ERs, and
- a false negative electrode (fn) if marked as SP-electrode but NOT showing ERs.

#### 2.7.4. Cross-check TD and TF analysis

Finally, we performed a cross-check of the ER results found by the TD and TF analysis in the patients for which SPES data of both types, high temporal resolution data and high dynamic range, were available. This includes: (a) association between ERs marked in the spike band in TF analysis with SP-electrodes when stimulating the SO-electrode, (b) calculation of the $ER_{50}$ electrodes for the total number of stimulus pairs of the TD data, and determining their association with the clinical SOZ electrodes. We computed sensitivity, specificity, PPV and NPV for seizure propagation and seizure onset zone, respectively.

## 3. Results

### 3.1. Overall patient results

For six patients (pt 1–6) SPES data were sampled at 2048 Hz in 64 channels allowing the TF analysis and association of ER counts with SOZ for different frequency bands. For eight patients (pt 1, 2, 7–12) data were recorded in up to 120 channels recorded at high dynamic range (22 bits) that allowed the TD analysis and association of ERs with seizure propagation. In two patients (pt 1, 2) both SPES data types were available.

For the six patients recorded at 2048 Hz the mean number of analyzed channels was 62 (±2). The median number of stimulated electrode pairs was 46 (range 16–55). The median number of electrodes in the SOZ was 5 (range 2–30). For the eight patients recorded at 22 bits a mean of 92 (±13) channels was analyzed. All patients had seizures with a focal gamma onset. For each patient a SO-electrode was marked. For detailed patient characteristics we refer to Table 1.

### 3.2. TF and TD analysis

In Fig. 1A a TF-domain ERSP image based on HHT is shown for one response electrode as presented to the observers. In Fig. 1B, the TD analysis of ERs for one electrode of ten responses to consecutive stimuli is shown. ERs were found in all patients, irrespective of the used analysis method.

#### 3.2.1. ER findings and association with SOZ and propagation

TF analysis for the six patients resulted in a kappa $\geqslant 0.4$ in five patients (pt 1–4, and 6) for the spike band, in six patients (pt 1–6) for the ripple band but in only one patient (pt 2) in the FR-band (four ERs in the FR-band on three electrodes), therefore the FR-band was excluded from further analysis. In Fig. 2 an example of the $ER_{norm}$ distribution in relation to the clinical SOZ is represented. Note that the SOZ is characterized by high values of $ER_{norm}$ (Fig. 2).

In three out of five patients with $k > 0.4$ (pt 1, 3 and 4) there was a significant difference between $ER_{norm}$ counts in- and outside the SOZ ($p < 0.05$, Mann–Whitney $U$) for the S-band and in three out of five patients (pt 1, 3 and 5) for the R-band ($p < 0.05$, Mann–Whitney $U$). See Fig. 3.

Similar results were found at individual patient level for electrodes marked as $ER_{50}$ electrodes. $ER_{50}$ electrodes were significantly associated with SOZ electrodes in the spike band in two patients (pt 1and 3; $p < 0.05$, Fisher exact) and in three patients in the ripple band (pt 1, 3 and 5; $p < 0.05$, Fisher exact).

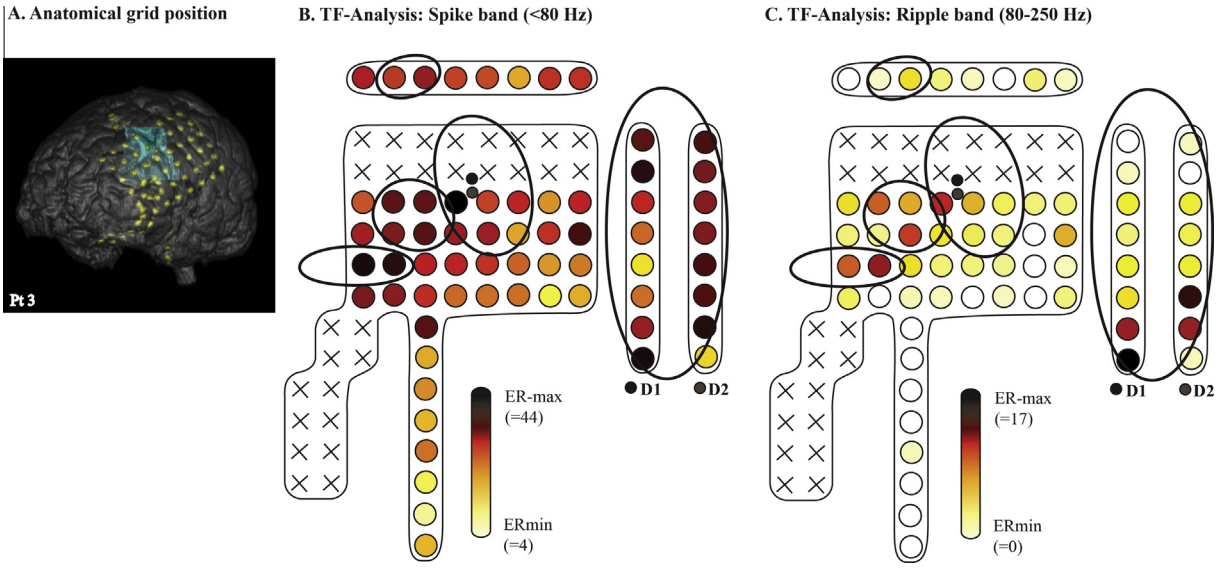


**Fig. 2.** Patient example (pt 3) of $ER_{norm}$ distribution. (A) MRI and CT merged images depicting the anatomical grid positions. (B) $ER_{norm}$ distribution in the spike band (<80 Hz) and relation with the SOZ (encircled areas). (C) $ER_{norm}$ distribution in the ripple band (80–250 Hz) and relation with the SOZ. *Note:* D1 and D2 are depth electrodes.

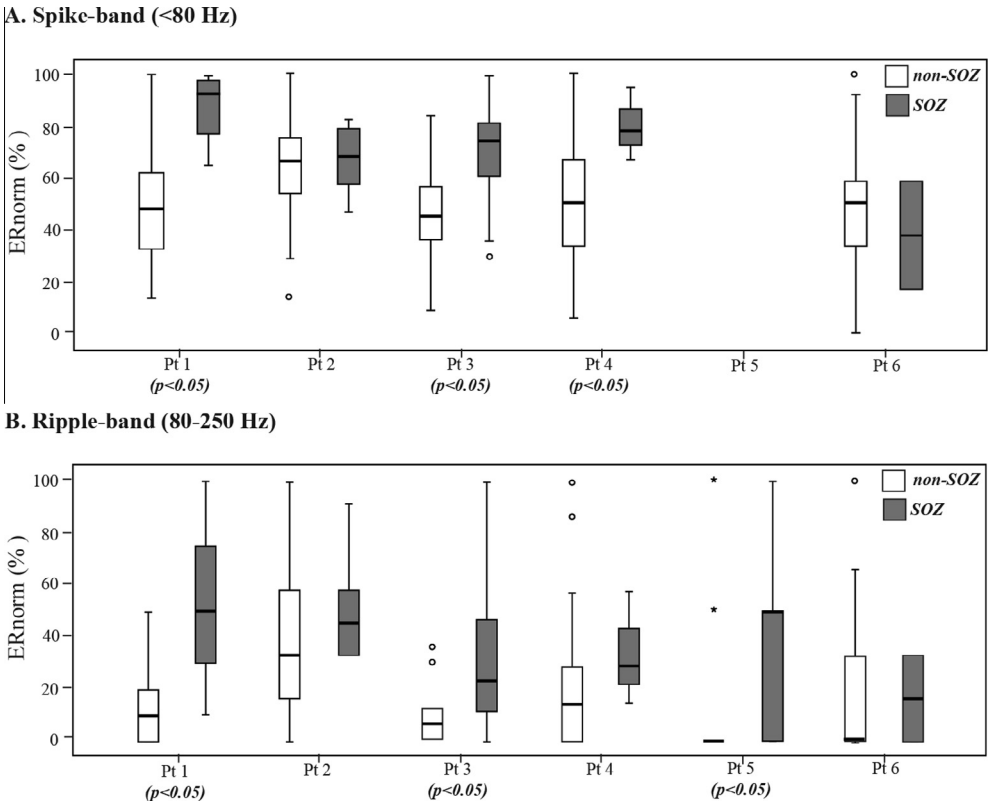


**Fig. 3.** Boxplots for difference in $ER_{norm}$ between channels in- and outside SOZ for (A) the spike band (<80 Hz); three patients (pt 1, 3 and 4) had a significant higher $ER_{norm}$ in the clinical SOZ. (B) The ripple band (80–250 Hz). In the ripple band a significant higher $ER_{norm}$ in the clinical SOZ was found for three patients (pt 1, 3 and 5).

At group level the association of $ER_{50}$ and the SOZ was significant for both the spike and ripple band ($p < 0.05$, Fisher exact) (Table 2).

In Fig. 4 an example is given for an individual patient (pt 1) of ERs detected using the TD method when stimulated in the SO-electrodes. Note that ERs are mostly present in SP-electrodes. ERs detected when stimulating in SO-electrodes were significantly associated with SP-electrodes in four patients (pt 8, 9, 10 and 12; $p < 0.05$, Fisher exact), and at group level ($p < 0.05$, Fisher exact) (Table 3).

### 3.2.2. Sensitivity and specificity of ER counts for SOZ and ERs for propagation

In the TF analysis group of six patients, we found a median sensitivity and specificity of $ER_{50}$ in the spike band for the SOZ of 87% and 44%, respectively. For the ripple band this sensitivity and

**Table 2**
Results of ER analysis in time–frequency (TF) domain and their relation with seizure onset.

| #Pt | TF/TD | # Elec | SOZ ($ER_{50}$) | | | | | | | | | |
|---|---|---|---|---|---|---|---|---|---|---|---|---|
| | | | Sens (%) | | Spec (%) | | PPV (%) | | NPV (%) | | *p*-Value* | |
| | | | S-band | R-band | S-band | R-band | S-band | R-band | S-band | R-band | S-band | R-band |
| 1 | TF | 61 | 100 | 75 | 56 | 95 | 14 | 50 | 100 | 98 | ***0.046*** | ***0.002*** |
| 2 | TF | 62 | 83 | 50 | 18 | 63 | 10 | 13 | 91 | 92 | 1.000 | 0.661 |
| 3 | TF | 64 | 87 | 23 | 56 | 100 | 63 | 100 | 83 | 60 | ***0.001*** | ***0.003*** |
| 4 | TF | 58 | 100 | 33 | 47 | 94 | 9 | 25 | 100 | 96 | 0.245 | 0.195 |
| 5 | TF | 64 | x | 55 | x | 83 | x | 40 | x | 90 | x | ***0.015*** |
| 6 | TF | 64 | 50 | 0 | 42 | 87 | 3 | 0 | 96 | 96 | 1.000 | 1.000 |
| Mean (±SD)/median (range) | | 62 (±2) | 87 (50–100) | 42 (0–75) | 44 (18–57) | 91 (63–100) | 9 (3–63) | 33 (0–100) | 96 (83–100) | 95 (60–98) | ***<0.001*** | ***<0.001*** |

Pt = patient, TF = time–frequency analysis, TD = time-domain analysis, # elec = the number of electrodes included in the analysis, Sens = sensitivity, Spec = specificity, PPV = positive predictive value, NPV = negative predictive value, S-band = spike band (<80 Hz), R-band = ripple band (80–250 Hz), SD = standard deviation. *Tested for association $ER_{50}$ with SOZ, using Fisher exact test (two-tailed), with $p < 0.05$ considered significant (in italic bold). *Note:* results for the FR-band in TF analysis are not reported because of the single finding in only one patient (pt 2).

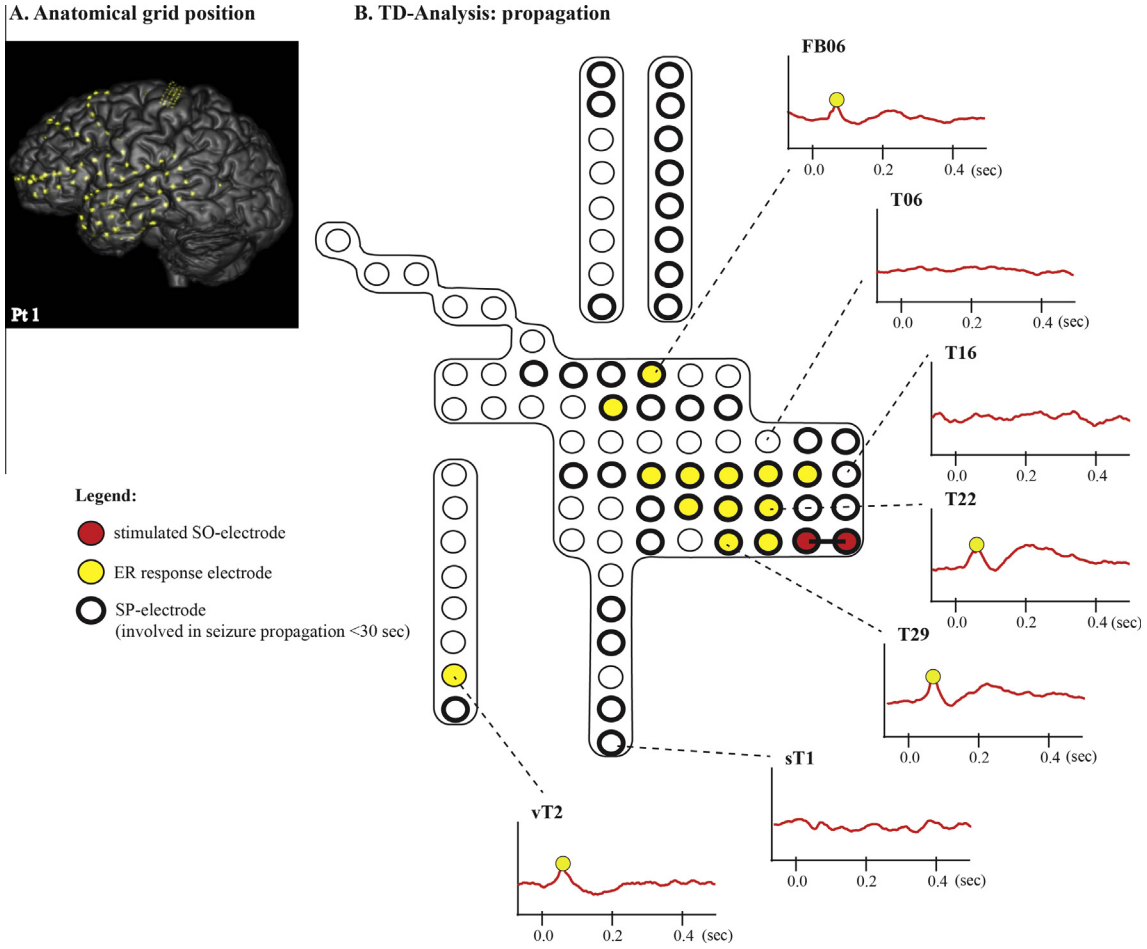


**Fig. 4.** Patient example (patient 1) of ER electrodes for stimulation in the SO-electrode (TD analysis) and the correlation with propagation (SP-electrodes). Included are examples of the ER waveforms in selected electrodes. Sensitivity here is 42%, specificity is 86%, and PPV and NPV are 40% and 87%, respectively.

specificity was 42% versus 91% (Table 2). Median sensitivity and specificity of ERs for the SP-electrodes was 32% and 94%, respectively in the TD analysis group of eight patients (Table 3).

### 3.2.3. Cross-check TD and TF analysis

In two patients (pt 1 and 2) we compared the results of both TD and TF analysis. Note that comparisons were for different datasets of the same patients. We found that:

– Association of evoked ERs with seizure propagation is significant for ER detected by TD analysis but not for ERs detected in the spike band by TF analysis in patient 1 ($p_{TD} = 0.011$ vs. $p_{TF} = 0.435$, Fisher exact). The opposite was found for the relation between evoked ERs counts and the SOZ; a significant association between $ER_{50}$ and the SOZ was found by TF analysis but not in TD analysis ($p_{TF} = 0.046$ vs. $p_{TD} = 1.000$, Fisher exact). Results for patient 2 were not significant (propagation:

**Table 3**
Results ER analysis in time-domain (TD) and relation with seizure propagation.

| #Pt | TD/TF | Propagation | | | | | | | | |
|---|---|---|---|---|---|---|---|---|---|---|
| | | # Elec | Threshold (μV) | Mean latency (ms) | Mean amplitude (μV) | Sens (%) | Spec (%) | PPV (%) | NPV (%) | *p*-Value* |
| 1 | TD | 102 | 120 | 46 | 301 | 42 | 86 | 40 | 87 | ***0.011*** |
| 2 | TD | 91 | 120 | 64 | 378 | 40 | 77 | 52 | 67 | 0.103 |
| 7 | TD | 88 | 90 | 35 | 262 | 24 | 93 | 44 | 84 | 0.066 |
| 8 | TD | 86 | 140 | 47 | 355 | 22 | 98 | 89 | 64 | ***0.003*** |
| 9 | TD | 77 | 120 | 44 | 443 | 60 | 84 | 47 | 90 | ***0.001*** |
| 10 | TD | 94 | 120 | 59 | 299 | 36 | 100 | 100 | 72 | ***0.000*** |
| 11 | TD | 118 | 140 | 44 | 286 | 19 | 94 | 55 | 76 | 0.067 |
| 12 | TD | 82 | 130 | 39 | 206 | 28 | 97 | 92 | 55 | **0.002** |
| Mean (±SD)/median (range) | | 92 (±13) | 123 (±16) | 47 (±10) | 316 (±73) | 32 (19–60) | 94 (77–100) | 54 (40–100) | 74 (55–90) | ***⩽0.001*** |

Pt = patient, TD = time-domain analysis, TF = time–frequency analysis, # elec = number of electrodes included in analysis, threshold = amplitude threshold used (see methods Section 2.6.2, step 2), mean amplitude = mean amplitude of ERs (baseline to peak), Sens = sensitivity, Spec = specificity, PPV = positive predictive value, NPV = negative predictive value, S-band = spike band (<80 Hz), R-band = ripple band (80–250 Hz), SD = standard deviation. *Tested for association ER response electrodes with SP-electrodes, using Fisher Exact test (two-tailed), with $p < 0.05$ considered significant (in italic bold).

$p_{TD} = 0.103$ vs. $p_{TF} = 0.263$, Fisher exact; SOZ: $p_{TF} = 1.00$ vs. $p_{TD} = 0.509$, Fisher exact). TD and TF analysis showed similar, low, sensitivity of ERs for propagation (range: 24–42%).
- ERs detected by TD analysis had a higher specificity for SP-electrodes than ERs detected by TF analysis (Fig. 5).
- Sensitivity values of $ER_{50}$ for the clinical SOZ were lower in both patients for TD (47% and 43%) compared to TF analysis (100% and 83%). Specificity values were comparable in patient 1 (54% vs 56%), but higher for the TD analysis in patient 2 (66% vs 18%) (Supplementary Table S1 in the Supplementary Material).

## 4. Discussion

The SOZ is more likely to be located in areas showing high counts of ERs evoked by SPES. ERs evoked by stimulation in seizure onset electrodes are more likely to occur in electrodes that show seizure propagation. ERs in the ripple band (80–250 Hz) exist and electrodes with high ER counts in the ripple band have a high specificity for SOZ channels. So, the analysis of ERs evoked by SPES can reveal aspects of pathology, even if the underlying stimulus–response relation is purely physiological. ERs, besides DRs, could assist in unraveling aspects of the epileptic network.

Based on our results, we cannot suggest a preferred general method of analysis for SPES early responses, as each method has its pro's and con's. For the detection of high frequency content time–frequency analysis is necessary, but results for the cross-check patients show that the TF method lacks specificity in the detection of lower frequency responses resulting from a single stimulation site like the SOZ. TD analysis of SPES yields robust responses with high specificity, but lacks the sensitivity needed to extract useful clinical information about the SOZ from the overall statistics of early responses.

### 4.1. Methodological aspects

We showed that SPES evokes ERs [0.0–0.1 s] with frequency features above the traditional 80 Hz. We used a HHT time–frequency analysis instead of a wavelet analysis as used in our previous study (van 't Klooster et al., 2011). A strength of time–frequency analysis is that it allows averaging in the frequency domain while retaining time information. The time resolution of wavelet analysis proved to be sufficient for DRs, since their relevant time interval lies between 0.15 s and 1.0 s after stimulation, and interference of the stimulus artifact is not an issue. The advantage of HHT is that it enables the detection of early ripple responses at a high time resolution, close to the stimulus artifact. HHT was successfully used in an earlier study by Kalitzin et al. (2012) to determine 'rippleness' of a signal (Kalitzin et al., 2012).

We are the first to find that SPES, with its low number of stimuli and low repetition rate, evokes ERs that can be associated with areas of seizure propagation, when stimulating the SOZ. The artifact removal algorithm applied in the time domain allowed us to detect ERs in a semi-automatic way, in spite of the low signal-to-noise ratio (SNR) of an average of only ten stimuli.

We were able to show an association between overall counts of ERs ($ER_{norm}$) and the SOZ at group level, and at individual level in four out of six patients. This finding seems to contradict the general finding of Valentín et al. (2002, 2005a,b) that early responses cannot localize epileptogenic cortex. In contrast to the studies of Valentin et al., in our study we count how often an electrode shows an ER response to stimulation throughout the SPES protocol and we relate this measure for the richness of connections to the underlying area to the SOZ (Valentín et al., 2002, 2005a,b).

Does this mean that we can propose ER analysis as a clinical tool? When it comes to predicting seizure propagation it should be noted that clinically identical seizures in semiology can originate from different foci. Our study is limited by the fact that we studied only one seizure per patient and looked at the resulting ERs when stimulating the corresponding SO-electrode. Including more data or more seizures per patient would have increased the statistical robustness and thus clinical usefulness of our results.

When it comes to predicting the SOZ the sensitivity and specificity, based on ER50, are insufficient for reliable prediction of the SOZ in individual patients. When we thresholded the $ER_{norm}$ values to obtain $ER_{50}$ electrodes, the sensitivity for the SOZ was relatively high (87%) for the spike band, but low for the ripple band (42%). Conversely, specificity is low (44%) for the spike band and high (91%) for the ripple band. Nevertheless information derived from ER counts can be added to that of pathological delayed responses, that have a high specificity and sensitivity (Valentín et al., 2002, 2005a,b; van 't Klooster et al., 2011) and can be established during the same SPES session.

Unlike ripples, fast ripples are described as primary pathological events (Staba et al., 2002; Worrell et al., 2004; Jirsch et al., 2006; Jacobs et al., 2008, 2010). We found only ERs in the fast ripple band in one patient. This low number of ERs in the fast ripple band cannot refute the assumption that ERs are purely physiological (Valentín et al., 2002; Lacruz et al., 2007; Rosenzweig et al., 2011), although the lack of fast ripples could be explained by the fact that HHT is less suitable for the noisy high frequency content above 250 Hz (Huang and Wu, 2008). Hardware requirements and the retrospective nature of this study resulted in small patient groups. Data suitable for both TF and TD analysis were not avail-

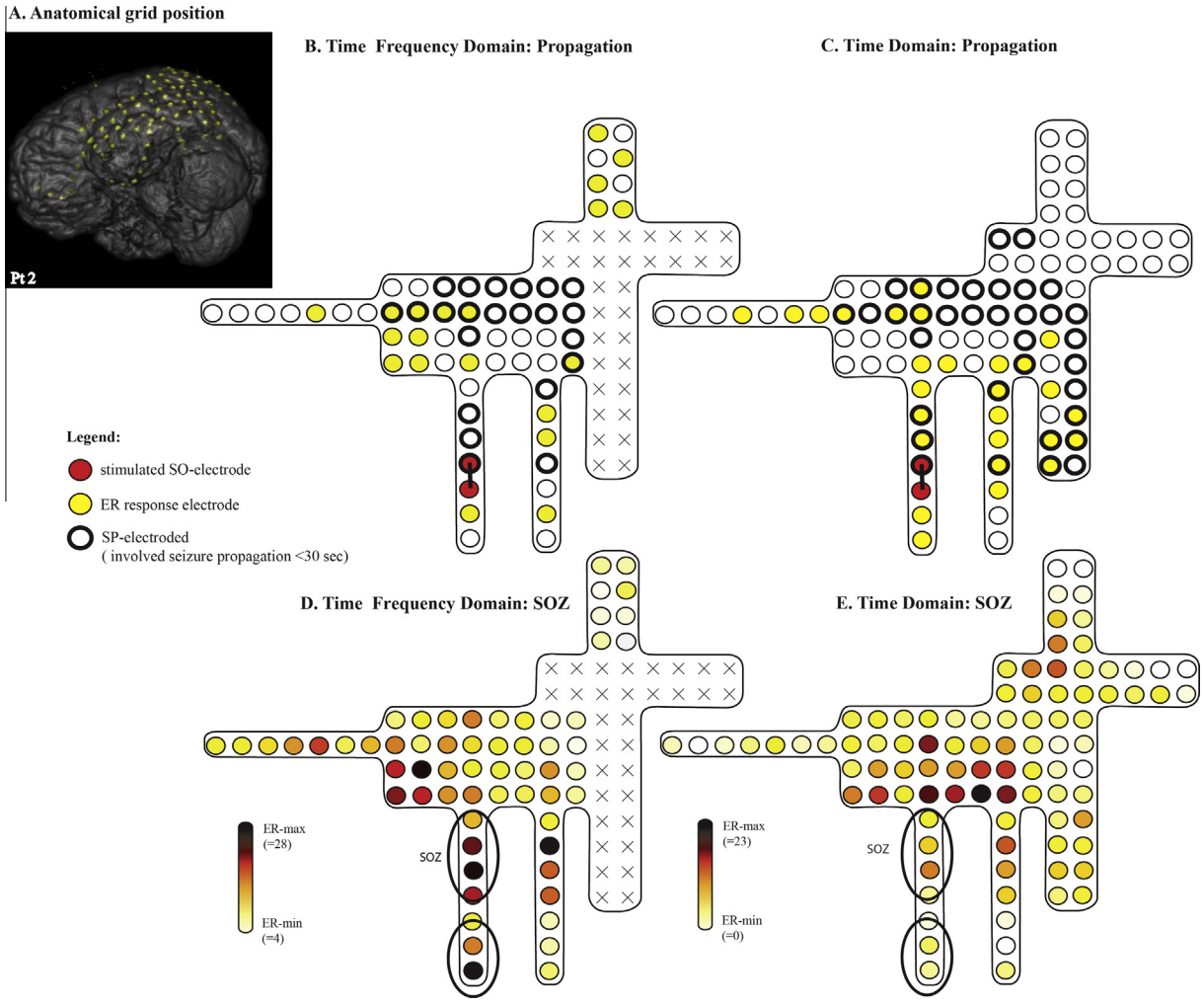


**Fig. 5.** Results of the cross-check of TF and TD analysis in one of the two patients (patient 2). (A) MRI and CT merged images depicting the anatomical grid positions. (B and C) TD and TF analysis show similar, low, sensitivity of ER responses for propagation. ERs detected by TD analysis had a higher specificity for SP-electrodes than ERcounts detected by TF analysis. (D and E) Sensitivity of $ER_{norm}$ for the clinical SOZ (encircled areas) are comparable for TD and TF analysis, but specificity is higher for the TD analysis.

able. Acquiring high frequency data at 2048 Hz meant a sacrifice of recorded ECoG channels to a maximum of 64. The choice of channels to retain was made during the clinical registration and was based on information about the SOZ then available. Capturing seizure propagation over the grid up to 30 s after onset was not considered when the selection of the 64 electrodes for 2048 Hz recordings was made. Interpretation of the comparison between the TF- and TD-based method is therefore hampered if propagation took place in sacrificed channels for the cross-check patients (see Fig. 5). Additionally, incomplete ECoG coverage of the cortex limits interpretation of results of TF and TD based methods in general.

All patients in the TD analysis showed propagation of both the seizure and the ER responses, not only local but also remote from the SOZ, several sulci and gyri away. We observed that seizures often showed substantial secondary propagation around the site they were initially propagated to. For ERs this was less often the case (see Figs. 4 and 5D; in the Supplementary Material a Video of an example where secondary ERs do occur is provided). As a result, sensitivity values of ERs for SP-electrodes are relatively low. Probably seizure activity produces more massive secondary activation of connecting fibers than SPES stimulation does. It could be worthwhile exploring local responses to additional SPES stimulation in the electrode where earliest ERs appear when stimulated in the SOZ.

Another limitation is that SPES recordings were not performed in a drug-free state for most patients, although AEDs were tapered during the ECoG monitoring session. Since AEDs may contain the spread of ERs across the cortical mantle, medication may have lowered the sensitivity of both the time-domain and the time–frequency domain method.

Both TD and TF approaches rely pre-dominantly on computational signal processing. These methods are, however, not fully automated as they still involve identification by a trained observer as a last step.

### 4.2. Relation with findings in literature

SPES relates to the CCEP stimulation protocol. In Enatsu et al. (2012) CCEPs were used to investigate the relation between evoked cortical responses and seizure propagation. Their CCEP protocol uses more stimuli (50–70) at a higher repetition rate (1 Hz) with pulses of shorter duration (0.3 ms), but an amplitude comparable to SPES (1–15 mA) (Enatsu et al., 2012a). Effectively, the injected charge would be equal to using 0.3–4.5 mA in SPES. Although this is lower (~50%), the signal-to-noise ratio for CCEPs is probably higher than for SPES, given the substantially higher amount of averages. Enatsu et al. (2012a) found no robust relation between seizure propagation and evoked responses. As in most CCEP stud-

ies, focus lied on amplitude and latency rather than occurrence and count of evoked responses. They found no significant difference between amplitude in electrodes with CCEPs and seizure propagation, compared to electrodes where only CCEPs without seizure propagation were observed (Enatsu et al., 2012a). Their conclusion that ictal propagation is not necessarily associated with functional connectivity is in contrast to our finding of a high specificity. An explanation could be that the lower SNR of SPES responses results in fewer detections, so fewer false positives with respect to seizure propagation compared to CCEP. On the other hand, the more powerful SPES stimulus current could ensure that a SPES response is more likely a true than a false positive with respect to seizure propagation, compared to CCEP.

On the matter of identification of the SOZ the CCEP literature shows a clear relation between enhanced CCEP response amplitudes when stimulation is inside the SOZ (called iCCEPs) compared to those when stimulating outside the SOZ (called nCCEPs) (Iwasaki et al., 2010; Enatsu et al., 2012a,b). There have been no reports on the association of the location of CCEP responses with the SOZ, independent of stimulation side. CCEP studies are characterized by a directional, functional connectivity analysis, whereas our SPES-study is characterized by a cumulative response analysis, rather the sum of all iCCEPs and nCCEPs. The CCEP directionality approach could be of interest in future SPES studies on delayed responses. Valentín et al. (2002, 2005a,b), e.g., showed that a focus in the temporal lobe is represented by tissue showing evoked delayed responses to a stimulus elsewhere, while in the frontal lobe stimulating the focus results in evoked delayed responses elsewhere (Valentín et al., 2002, 2005a,b).

Recently, Boido et al. (2014) looked specifically at directionality, using a different CCEP protocol (30 pulses at 1 Hz, 2 ms, 4 mA; delivered in depth electrodes (SEEG) with 1.5 mm separation). Note that here current density values exceed those of the CCEP studies mentioned earlier, and also of SPES. They defined electrodes as primarily receivers, activators or bidirectional contacts. Their receivers resemble roughly the $ER_{50}$ electrodes in our study. They did not find, however, an association between primary receiver electrodes and SOZ. Their activators did not show an association with SOZ, nor seizure propagation. However, bidirectional connectivity was a prevalent feature for contacts included in the epileptogenic focus (Boido et al., 2014). The large differences in stimulus parameters and detection thresholds hamper interpretations of the mismatch between their and our results. Therefore, studies that combine CCEP and SPES protocols and analysis methods will be important to better understand the underlying physiological mechanisms of the responses each protocol evokes. Evaluating both CCEP and SPES early and delayed responses, including directionality, in the same epilepsy patient could increase the clinical yield of intracranial electrical stimulation.

### 4.3. Conclusions

To conclude, we found that analysis of ERs evoked by SPES reveals information about the pathology, manifested by the localization of the SOZ in areas of high ER counts and by the ability of ERs to predict seizure propagation. ERs information could be added to that of DRs to improve pre-operative mapping of epileptogenic cortex and the epileptic network. Larger studies, including prospective studies, are needed to establish the full clinical potential of SPES.

## Acknowledgements

Ms. van 't Klooster is supported by the Dutch Epilepsy Foundation, grant number 2012–04. Mr. Hebbink is supported by the ZonMW Translational Research grant 95104015. Ms. Zijlmans is supported by the Rudolf Magnus Institute Talent fellowship.

*Conflict of interest:* The authors report no conflict of interest.

## Appendix A. Supplementary data

Supplementary data associated with this article can be found, in the online version, at http://dx.doi.org/10.1016/j.clinph.2015.07.031.

## References

Alarcon G. Electrophysiological aspects of interictal and ictal activity in human partial epilepsy. Seizure 1996;5:7–33.
Alarcon G, Guy CN, Binnie CD, Walker SR, Elwes RD, Polkey CE. Intracerebral propagation of interictal activity in partial epilepsy: implications for source localisation. J Neurol Neurosur Psychiatry 1994;57:435–49.
Boido D, Kapetis D, Gnatkovsky V, Pastori C, Galbardi B, Sartori I, et al. Stimulus-evoked potentials contribute to map the epileptogenic zone during stereo-EEG presurgical monitoring. Hum Brain Mapping 2014;35:4267–81.
Delorme A, Makeig S. EEGLAB: an open source toolbox for analysis of single-trial EEG dynamics including independent component analysis. J Neurosci Methods 2004;134:9–21.
Enatsu R, Jin K, Elwan S, Kubota Y, Piao Z, O'Connor T, et al. Correlations between ictal propagation and response to electrical cortical stimulation: a cortico-cortical evoked potential study. Epilepsy Res 2012a;101:76–87.
Enatsu R, Piao Z, O'Connor T, Horning K, Mosher J, Burgess R, et al. Cortical excitability varies upon ictal onset patterns in neocortical epilepsy: a cortico-cortical evoked potential study. Clin Neurophysiol 2012b;123:252–60.
Huang NE, Wu Z. A review on Hilbert-Huang transform: method and its applications to geophysical studies. Rev Geophys 2008;46:1–23.
Iwasaki M, Enatsu R, Matsumoto R, Novak E, Thankappen B, Piao Z, et al. Accentuated cortico-cortical evoked potentials in neocortical epilepsy in areas of ictal onset. Epileptic Disord 2010;12:292–302.
Jacobs J, LeVan P, Chander R, Hall J, Dubeau F, Gotman J. Interictal high-frequency oscillations (80–500 Hz) are an indicator of seizure onset areas independent of spikes in the human epileptic brain. Epilepsia 2008;49:1893–907.
Jacobs J, Zijlmans M, Zelmann R, Chatillon CE, Hall J, Olivier A, et al. High-frequency electroencephalographic oscillations correlate with outcome of epilepsy surgery. Ann Neurol 2010;67:209–20.
Jirsch JD, Urrestarazu E, LeVan P, Olivier A, Dubeau F, Gotman J. High-frequency oscillations during human focal seizures. Brain 2006;129:1593–608.
Kalitzin S, Zijlmans M, Petkov G, Velis D, Claus S, Visser G, et al. Quantification of spontaneous and evoked HFO's in SEEG recording and prospective for pre-surgical diagnostics. Case study. Engineering in Medicine and Biology Society (EMBC), 2012 Annual International Conference of the IEEE2012. p. 1024–7.
Lacruz ME, García Seoane JJ, Valentin A, Selway R, Alarcón G. Frontal and temporal functional connections of the living human brain. Eur J Neurosci 2007;26:1357–70.
Matsumoto R, Kinoshita M, Taki J, Hitomi T, Mikuni N, Shibasaki H, et al. In vivo epileptogenicity of focal cortical dysplasia: a direct cortical paired stimulation study. Epilepsia 2005;46:1744–9.
Matsumoto R, Nair DR, LaPresto E, Bingaman W, Shibasaki H, Luders HO. Functional connectivity in human cortical motor system: a cortico-cortical evoked potential study. Brain 2007;130:181–97.
Matsumoto R, Kunieda T, Ikeda A. In vivo investigation of human brain networks by using cortico-cortical evoked potentials. Brain Nerve 2012a;64:979–91.
Matsumoto R, Nair DR, Ikeda A, Fumuro T, Lapresto E, Mikuni N, et al. Parieto-frontal network in humans studied by cortico-cortical evoked potential. Hum Brain Mapp 2012b;33:2856–72.
Noordmans HJ, Rijen PCV, Veelen CWMV, Viergever MA, Hoekema R. Localization of implanted EEG electrodes in a virtual-reality environment. Comput Aided Surg 2002;258:241–58.
Rilling G, Flandrin P, Gonçlavès P. On empirical mode decomposition and its algorithms. In: Proceedings of the IEEE-EURASIP workshop on Nonlinear Signal and Image Processing (NSIP); 2003. p. 8–11.
Rosenzweig I, Beniczky S, Brunnhuber F, Alarcon G, Valentin A. The dorsal hippocampal commissure: when functionality matters. J Neuropsychiatry Clin Neurosci 2011;23:E45–8.
Saito T, Tamura M, Muragaki Y, Maruyama T, Kubota Y, Fukuchi S, et al. Intraoperative cortico-cortical evoked potentials for the evaluation of language function during brain tumor resection: initial experience with 13 cases. J Neurosurg 2014;121:827–38.
Spencer SS. Cortical and intercortical seizure spread. In: Meldrum BS, Ferrendelli JA, Wieser HG, editors. Anatomy of epileptogenesis. Libbey; 1988.
Staba RJ, Wilson CL, Bragin A, Fried I, Engel Jr J. Quantitative analysis of high-frequency oscillations (80–500 Hz) recorded in human epileptic hippocampus and entorhinal cortex. J Neurophysiol 2002;88:1743–52.
Valentín A, Anderson M, Alarcón G, Seoane JJG, Selway R, Binnie CD, et al. Responses to single pulse electrical stimulation identify epileptogenesis in the human brain in vivo. Brain 2002;125:1709–18.
Valentín A, Alarcón G, García-Seoane JJ, Lacruz ME, Nayak SD, Honavar M, et al. Single-pulse electrical stimulation identifies epileptogenic frontal cortex in the human brain. Neurology 2005a;65:426–35.

Valentín A, Alarcón G, Honavar M, García Seoane JJ, Selway RP, Polkey CE, et al. Single pulse electrical stimulation for identification of structural abnormalities and prediction of seizure outcome after epilepsy surgery: a prospective study. Lancet Neurol 2005b;4:718–26.

van 't Klooster MA, Zijlmans M, Leijten FS, Ferrier CH, van Putten MJ, Huiskamp GJ. Time-frequency analysis of single pulse electrical stimulation to assist delineation of epileptogenic cortex. Brain 2011;134:2855–66.

Worrell GA, Parish L, Cranstoun SD, Jonas R, Baltuch G, Litt B. High-frequency oscillations and seizure generation in neocortical epilepsy. Brain 2004;127:1496–506.

Zijlmans M, Flanagan D, Gotman J. Heart rate changes and ECG abnormalities during epileptic seizures: prevalence and definition of an objective clinical sign. Epilepsia 2002;43:847–54.